Chapter 11
An Optical Technique for Measuring Transient and Residual Interstory Drift as Seismic Structural Health Monitoring (S^2HM) Observables

David B. McCallen and Floriana Petrone

Abstract Building interstory drift (ID), which is a measure of the relative displacement between two successive floors in a vibrating building, is a key response parameter utilized in both seismic design and post-earthquake damage assessments. To this point in time, there has been no accepted methodology or sensor technology for reliable and accurate direct measurements of building drift. Indirect measurement of drift, through signal processing and double integration of accelerometer data, is fraught with challenges, particularly when inelasticity-induced permanent drifts occur. In this paper, recent developments toward a new optically-based technique for measurement of both transient interstory drift (TID(t)) and residual interstory drift (RID) are described. The ability of a newly designed laser-based optical sensor system to directly measure interstory drift is demonstrated through experimental and model-based evaluations. This sensor technology has progressed to the point where practical application is feasible as an enabling S^2HM technology.

Keywords SHM · Seismic monitoring · Interstory drift · Damage detection · Optical sensor development · Structural damage

11.1 Introduction

Traditional techniques for measuring structural system response under vibrations rely on strong motion accelerometer instrumentation [20]. A number of research works and practical applications have demonstrated the capability of accelerometer-based systems to provide data for structural vibration monitoring and modal identification [9, 13, 18]. However, for evaluating the performance of a building after major seis-

D. B. McCallen (✉)
Department of Civil and Environmental Engineering, University of Nevada,
1664 North Virginia St, Reno, NV, USA
e-mail: dmccallen@unr.edu

D. B. McCallen · F. Petrone
Energy Geosciences Division, Lawrence Berkeley National Laboratory,
1 Cyclotron Road, Berkeley, CA, USA

M. P. Limongelli and M. Çelebi (eds.), *Seismic Structural Health Monitoring*, Springer Tracts in Civil Engineering, https://doi.org/10.1007/978-3-030-13976-6_11

mic events, structural performance parameters such as peak interstory drift (PID) and residual interstory drift (RID) become key measures to assess structural damage and inform decisions on continuity of operations and safety of occupancy. Determining interstory drift from recorded acceleration response histories requires significant data processing and is subject to a number of technical challenges. Historically, ID has been computed by double integration of acceleration time histories to obtain floor absolute displacements, which in turn are differenced to obtain the relative displacement between two adjacent floors. Signal processing for baseline correction and bandpass filtering can be "delicate and sometimes subjective" [22], and the dynamic rotations of the accelerometer instrument, which are not typically measured/known, may be necessary to reliably compute displacements from acceleration records if rigid body rotations occur [23, 24].

Optical techniques for measuring building geometry based on photogrammetry have also been investigated and, under controlled laboratory conditions, have experimentally demonstrated an ability to achieve positional accuracy on the order of 0.5 cm with consumer grade single-lens-reflex cameras [7]. However, limitations for practical applications have been identified in the precision of the camera, the quality of the photos, the functionality of the photo-processing software as well as the lack of a formal method for assessing the accuracy of geometric measurements [8]. The demonstration of such methods in a more cluttered post-earthquake environment needs to be evaluated to understand the full potential for assessing for example residual drift in a damaged building.

More recently, research works have examined the potential of Micro Electro Mechanical Systems (MEMS) to detect structural damage. Hou et al. [11] have proposed an optimal layout of MEMS inclinometers to maximize the measurement accuracy in structures exhibiting elastic and inelastic deformations, but with experimental testing limited to single structural components under static loading conditions. Inclinometers typically rely on a constant gravity field for their measurement principle and imposition of earthquake accelerations in three dimensions can in fact disrupt rotation measurements. Hsu et al. [12] have developed MEMS seismometers to identify damage in building structures, but with the limitation of having the same post-processing criticalities highlighted for classical acceleration-based monitoring systems.

In the early development of the optical sensor described herein, the authors explored another optical technique based on the use of high-quality CCD cameras to directly measure building drift displacements but the repeatability and accuracy was less than expected.

In this context, it would be highly desirable to have a practical method for directly measuring interstory drift to validate computational models of existing buildings, to assess the attainment or exceedance of limit states, and to inform immediate post-earthquake damage assessments and decisions on emergency response. Critical facilities such as hospitals, emergency response centers and data/financial centers would benefit substantially from rapid data on potential damage levels, as well as potential damage locations, immediately after a major earthquake.

Rapid advancements in sensor technologies and agile communications are creating new opportunities for transformational approaches to S^2HM. Driven by applications in many diverse fields (e.g. robotic machine control, autonomous vehicles etc.), optically-based sensor systems have undergone significant advancement in the past decade. Optically-based systems can have inherent advantages, including the extremely short latency of the underlying physics and the ability to perform high resolution measurements. Together, these features can result in very broad frequency band and high-fidelity measurements. In addition, the revolution underway in wireless communications and the Internet of Things (IOT) is providing an entirely new paradigm for command and control of sensor systems and for expedient exfiltration of data. Early research studies have investigated the potential of employing optical sensors and lasers to measure the dynamic response of structural systems [6, 25]. These works have also highlighted the need to account for rotations associated with structural member deformations that can have a significant impact on laser light propagation in determining interstory drift [21, 22].

In this paper a newly developed optical sensor for monitoring building earthquake response is described and the performance of the sensor is demonstrated through the data obtained from a comprehensive, multi-testbed, experimental campaign. This technology provides, for the first time, a means for obtaining direct, broad-band, high fidelity measurements of building interstory drift. The developed sensor technology can also readily be incorporated into advanced building monitoring frameworks such as described in Celebi et al. [3] and Celebi [4].

A number of existing seismic design standards utilize interstory drift to define building limit states, to establish limits on PID, which is the maximum TID(t) obtained over the duration of the earthquake, and to measure potential building damage states after a major earthquake event, as summarized in Table 11.1. Despite the prevalent use of drift as a key response parameter and damage observable, there remarkably has been no robust and reliable technique developed to directly measure drift displacements.

Table 11.1 International codes and standards utilizing interstory drift as a performance or damage observable

Specification	Standard
Definition of system limit states in terms of PID	ASCE 43-05
Definition of system maximum allowable Interstory drift in terms of PID	Eurocode EN1998-1 New Zealand standard NZS-1170.5 Tall building initiative TBI 2.01
Definition of system damage states in terms of RID	FEMA P58-1 Tall building initiative TBI 2.01
PID = Maximum TID(t) over the duration of the earthquake event, RID = TID(t) as $t \rightarrow \infty$	

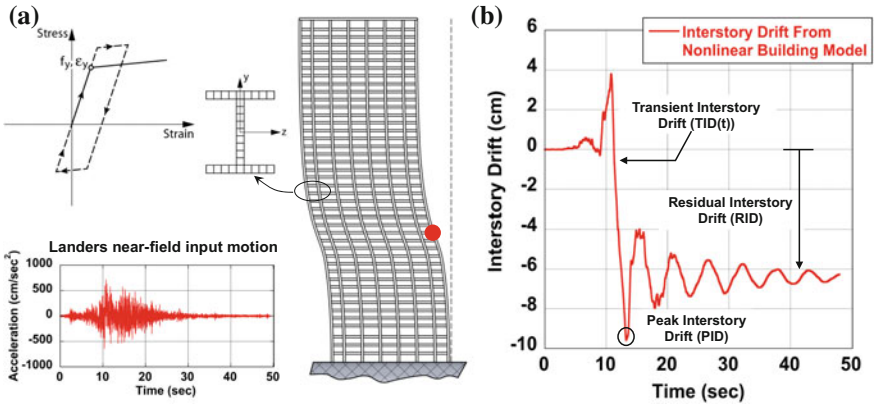

Fig. 11.1 Interstory drift from a representative nonlinear building model. **a** Deformed shape of a 40-story building FEM [14] subjected to Landers input motion [5]; **b** graphical representation of TID(t), PID and RID

11.2 Optically-Based Measurements for Interstory Drift

A graphical representation of TID(t), PID and RID is provided in Fig. 11.1, where a synthetic interstory drift waveform obtained from a 40-story nonlinear steel frame building model subjected to strong near-field motions is shown. The 40-story building was designed for UBC zone 3 and is characterized by a story height of 4 m in all intermediate floors, and 5.5 m in the first and top floor (Fig. 11.1a). The detailed building model utilizing finite deformation, fiber beam elements with elasto-plastic kinematic hardening [14] was subjected to near-fault Landers earthquake motions [5]. As evident in Fig. 11.1b, the interstory drift waveform at approximately one-third of the building height resulted in a significant PID (about 2.5% drift ratio) as well as in a substantial RID (about 1.5% drift ratio) as a result of building system yielding and inelastic deformation.

Although existing codes and standards only refer to PID and RID, the most effective system for drift measurement should be capable of measuring PID, RID and TID(t). In fact, for structures with potential cyclic degrading response features, e.g. reinforced concrete undergoing inelastic action associated with many cycles, it would be desirable to define a drift damage measure that includes aspects of the duration of loading and number of cycles at a given amplitude of drift, which can only be expressed by TID(t) [2, 10].

A new *Discrete Diode Position Sensor* (DDPS) has recently been developed to allow full broad-band measurements of interstory drift [15]. This technology utilizes a carefully configured geometric array of light-sensitive photodiodes to track the instantaneous position of an incident laser beam, as shown in Fig. 11.2c. The prototype DDPS adopted 92 diodes arranged in a staggered rectangular array configured such that the laser beam is always incident on one or more diodes. A sampling rate of

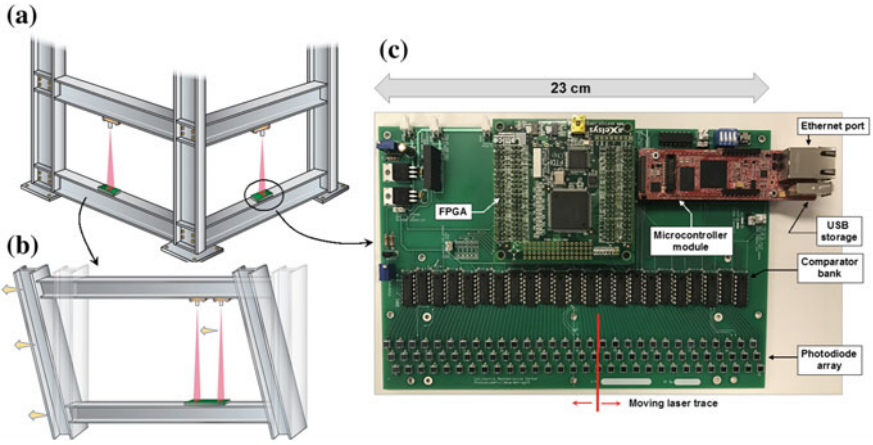

Fig. 11.2 Discrete Diode Position Sensor (DDPS) technology. **a** DDPS mounting for in-plane drift measurement; **b** translation of an incident laser line source on a DDPS during in-plane drift; **c** board mounted DDPS with moving laser trace illustrated

384 times per second is used, which corresponds to a Nyquist frequency of 192 Hz. To increase the position localization accuracy, the three linear arrays of diodes are staggered so that the active areas of the diodes overlap by D/3, where D is the nominal width of the diode active area.

As the laser line trace moves back and forth with in-plane motion, the position of the laser is theoretically determined to within D/6, and the readout of the sensor is a quantized set of displacements that increment by D/3. The width of the active area of the diodes adopted in this study is approximately 0.29 cm, which would yield a theoretical measurement error of approximately 0.05 cm. However, experimental tests on the as-built DDPS indicated that the realized position error is closer to 0.10 cm [15] due to slight positioning errors of the individual diodes, effective diode areas resulting from some dimensional variability, and the finite dimension of the diffracted laser trace.

As a building undergoes earthquake excitation, the laser beam translates back and forth across the photodiodes, which individually generate a voltage when hit by incident laser light, see Fig. 11.2a and b. The laser beam is diffracted through an optic to create a line projection as opposed to a point projection on the diode array. The resulting line trace is illustrated schematically in Fig. 11.2c, but in practice the line trace is much wider so that the laser will not move off the diode array when transverse displacements occur in a building undergoing vibration in three dimensions [15]. By rapidly sampling the photodiode voltages across the entire photodiode array using a Field Programmable Gate Array (FPGA), the instantaneous position of incidence of the laser line source on the sensor is determined and translated into a direct measurement of story drift displacement.

The next section of this article summarizes the results of a three-phase experimental campaign aimed at establishing DDPS dynamic performance.

11.3 Sensor Testbeds and Experimental Evaluation of DDPS Performance

Three experimental testbeds have been utilized in the DDPS development activities.

11.3.1 Testbed #1: DDPS Inherent Measurement Performance

The first testbed consisted of an automatically controlled precision motion table that could impart representative interstory drift motions to evaluate the inherent measurement performance of a DDPS as indicated in Fig. 11.3. This testbed allowed the evaluation of the fundamental ability and resolution of the DDPS to measure TID(t), PID, and RID. The experimental process consisted of imposing representative building drifts on the testbed and comparing DDPS measurements to the ground truth of imposed drifts. For example, for the synthetic drift in Fig. 11.1b, the imposed drift versus the DDPS measurement of the imposed drift and the resulting DDPS error are shown in Fig. 11.4a and b, respectively.

As illustrated in Fig. 11.4a and b, the DDPS very accurately measured all the key features of the entire imposed interstory drift waveform, with the sensor exhibiting a drift displacement measurement error of approximately 0.1 cm. This experimental

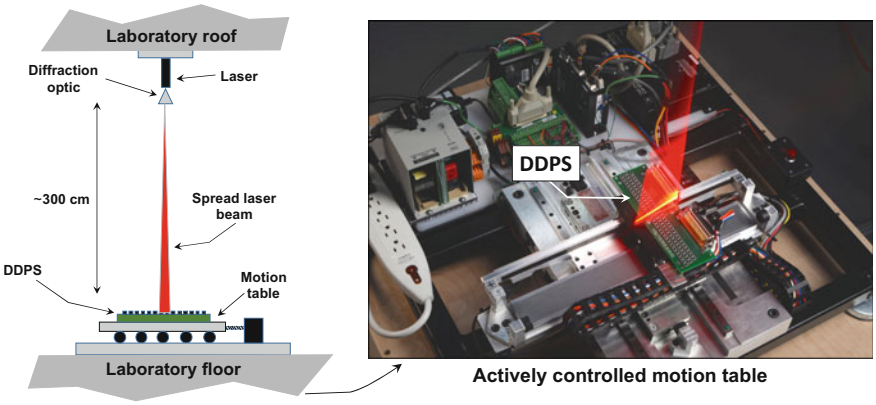

Fig. 11.3 Sensor testbed #1: automatically controlled motion table for generating representative ceiling-to-floor drift displacements

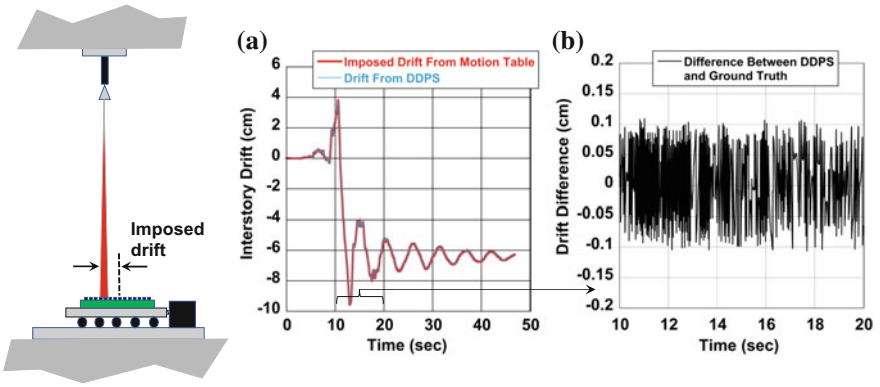

Fig. 11.4 Testbed #1 data on DDPS measurements. **a** Imposed motion versus DDPS measurements; **b** DDPS error

set-up provided the first data on DDPS performance and established that the accuracy of the DDPS met the sensor design objectives.

11.3.2 Testbed #2: DDPS Performance on a Laboratory Planar Frame

The second testbed consisted of a laboratory scale two-story moment frame with an automatically controlled stepper motor for imposing specified earthquake motions at the base of the frame, as shown in Fig. 11.5. Ground truth drift was acquired by tensioned wires connected to an adjacent diagnostic tower with string potentiometers for measuring wire extension and contraction, thus providing a direct measure of absolute story displacements. The objective of this experimental set-up was to evaluate the DDPS under more realistic structural dynamic conditions and include the additional challenge of developing a correction to account for the local structural member rotations at the mounting point of the laser. As documented in McCallen et al. [15], the local rotation of the structural members where the laser is mounted can have a substantial effect on the observed measurement of interstory drift. From the deformed shape of a frame subject to horizontal forces (Fig. 11.5), it is noted that the actual drift at each time step $\Delta_{Drift}(t)$ is computed as $\Delta_{Drift}(t) = \Delta_{Observed}(t) + \Delta_{Rotation}(t)$, where $\Delta_{Observed}(t)$ is the drift measured directly by the horizontal DDPS and $\Delta_{Rotation}(t)$ is the laser trace translation caused by the local rotation at the laser mounting point. $\Delta_{Rotation}(t)$ can be calculated as $\Delta_{Rotation}(t) = \Theta_{Laser}(t) \cdot H$, where $\Theta_{Laser}(t)$ is the local rotation at the laser mount location and H the distance between the laser and the horizontal DDPS. The unknown $\Theta_{Laser}(t)$ is then derived based on the measurements provided by a horizontal laser beam impinging onto the vertically mounted DDPS, as $\Theta_{Laser}(t) = \Delta_{Vertical}(t) \big/ W$, where $\Delta_{Vertical}(t)$ is the vertical translation

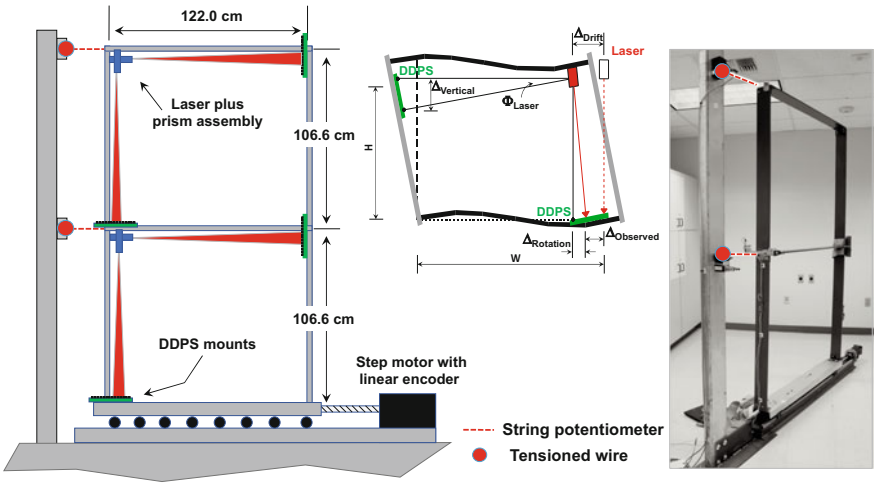

Fig. 11.5 Sensor testbed #2: scale model two story moment frame with an automatically controlled stepper motor for imposing earthquake motion

of the horizontal laser beam measured on the vertical DDPS and W is the distance between the location of the horizontally propagating laser and the vertical DDPS. Therefore, for a typical mounting configuration, such as that illustrated in Fig. 11.5, the deployment of a horizontal laser and vertical DDPS, in addition to the vertical laser and horizontal DDPS, allows calculating the local rotation of the vertical laser and appropriately correcting the drift measured by the vertical laser on the horizontal DDPS.

The experimental frame was subjected to ground motions from actual earthquake records and the story displacements were measured by the string potentiometers (taken as ground truth) and DDPS at each floor level. For applied El Centro earthquake input motion (PEER database [17]), the frame displacement drift waveforms are shown in Fig. 11.6a.

For Testbed #2, the DDPS error was ~0.15–0.2 cm (Fig. 11.6b). Based on a simple error analysis that accounts for both the error in the direct drift measurement on the horizontal DDPS and the error in the laser rotation measurement on the vertical DDPS, the maximum error is expected to be on the order of twice the error from a single sensor measurement. The observed peak sensor errors of ~0.18–0.2 cm were therefore in theoretical agreement with the expected maximum sensor error. Throughout the two-story frame experimental testing, it was confirmed that the DDPS error was essentially independent of drift amplitude, which was theoretically to be expected, and the DDPS hardware was robust against any adverse effects of the imposed shaking and vibration on the sensor components. Overall, the DDPS exhibited an ability to accurately measure the transient drift waveforms in terms of both frequency content and amplitude.

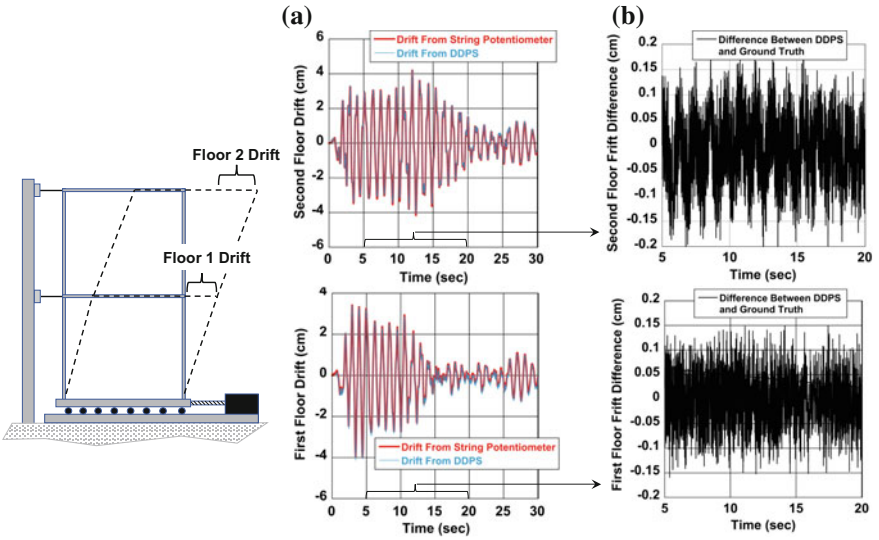

Fig. 11.6 Testbed #2 data on DDPS measurements. **a** DDPS versus ground truth; **b** DDPS error

11.3.3 Testbed #3: DDPS Performance on a Scaled 3D Steel Frame Under Bidirectional Excitation

The third testbed consisted of a significantly larger and more representative 1/3 scale steel frame structure mounted on a large hydraulic shake table at the University of Nevada, Reno Earthquake Engineering Research Laboratory (Fig. 11.7). The test set-up included a full suite of tensioned wire diagnostics to measure ground truth drift displacements at all three floor levels as well as accelerometers at each floor level. The test frame was subjected to bi-axial earthquake motions from representative measured earthquake records.

The objective of this testing set-up was to validate a second generation, single-board, DDPS design and demonstrate sensor performance at a scale more representative of actual building field conditions. For the Nevada experiments a large suite of tests were executed starting with scaled-down, low amplitude motions and progressing to increasingly higher motions until the earthquake input motions were scaled by up to 250%. This allowed evaluation of DDPS hardware performance under very strong shaking at larger optical distance ranges (laser-to-sensor) than previous laboratory structure experiments.

Representative data from the Nevada shake table experiments are shown in Fig. 11.8a for imposed El Centro earthquake ground motions scaled by 250%. As with previous tests, the drift measurements from the DDPS system deployed on the frame exhibited excellent agreement with ground truth drift and the DDPS peak error was on the order of 0.2 cm (Fig. 11.8b). It should be noted that in these larger-scale experiments the tensioned wires had a much longer span than in previous tests and

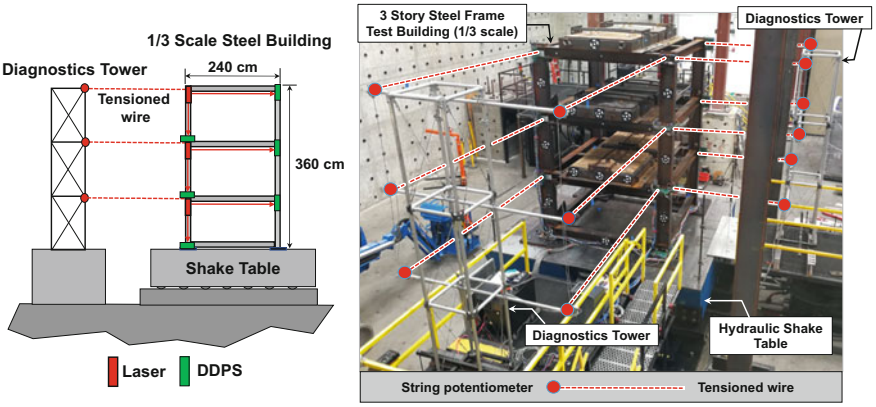

Fig. 11.7 Sensor testbed #3: 1/3 scale three story steel frame mounted on a hydraulic shake table

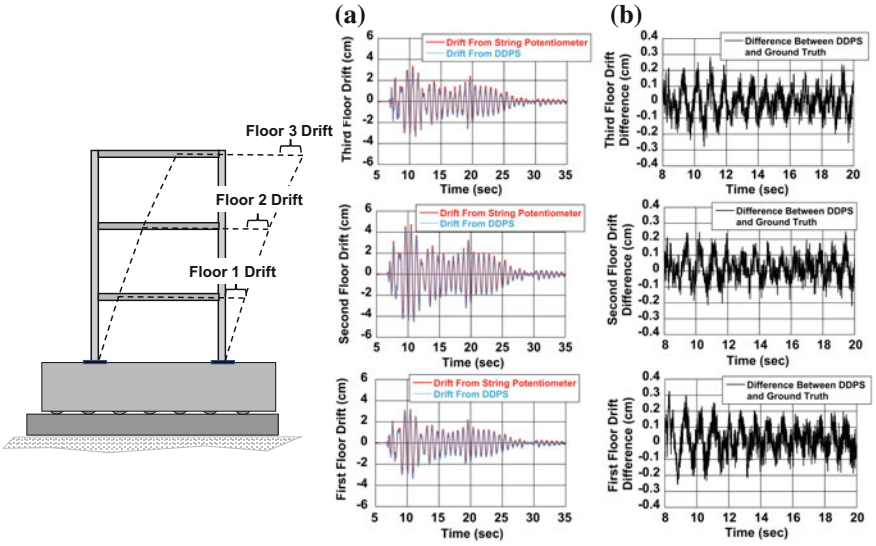

Fig. 11.8 Testbed #3 data on DDPS measurements. **a** DDPS versus ground truth and **b** DDPS error

some error in the ground truth measurements due to wire dynamic vibration could be expected. In the Nevada experiments the DDPS worked flawlessly throughout the entire test sequence under the very strong shaking associated with 250% ground motions. This provided significant performance data on the ruggedness of the DDPS board design.

The integrated set of experiments performed over the past two years on the three testbeds have provided significant data to validate the performance of a DDPS system for drift measurements. Looking forward to deployment on full-scale structures, it is instructive to evaluate how the drift displacements measured on the three testbeds

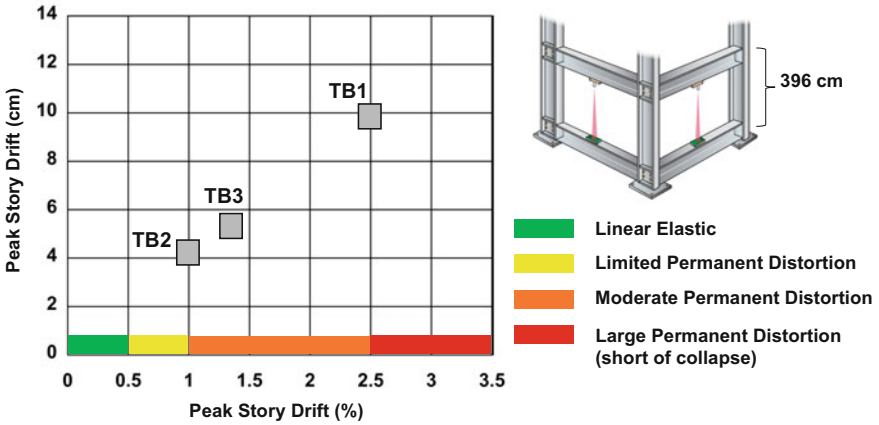

Fig. 11.9 Drift defined limit states for a representative steel moment frame (from ASCE/SEI 43-05 [1]) and drifts measured on each the three DDPS experimental testbeds (TB1, TB2, TB3)

compare to representative drifts that could be achieved on an actual full-scale building undergoing strong earthquake motions.

Figure 11.9 illustrates the drift for a representative steel moment frame with a story height of 366 cm (12 ft) and includes representation of limit states in accordance with the maximum drift limits provided in the ASCE/SEI 43-05 [1] for nuclear facilities. Standard 43-05 provides four drift-defined states for steel moment frames, which describe four regimes of system response ranging from linear elastic to large permanent distortion short of collapse as indicated in Fig. 11.9. The peak drifts measured in the experiments performed on each of the three testbeds are also indicated in Fig. 11.9 (TB1 = Testbed #1, TB2 = Testbed #2, TB3 = Testbed #3). The experimentally measured drifts from the scaled experiments are commensurate with the drift that would be achieved in a full-scale structure when significant inelastic behavior is occurring. This supports the fact that a DDPS can measure representative large drift displacements in a full-scale structure, and it should be noted that the range of the DDPS, defined by the length of the diode array (i.e. the 23 cm length in Fig. 11.2), can be adjusted to the maximum drift that might be achieved in a particular structure.

11.4 Model-Based Simulations of Sensor System Performance

As an integral part of the DDPS development, finite element models (FEMs) have been employed throughout the sensor design and testing process in order to build validated confidence in the ability of simulation models to predict deployed sensor system performance. Ultimately, confidence in a simulation-based tool for sensor

system design will be a key capability for appropriately designing sensor systems for specific structure configurations and is thus an important element of the overall technology base.

To help explore model-based predictions, computational models of testbed #2 and testbed #3 structures were constructed in the *OpenSees* [16] program environment. The test structures were modeled with combinations of beam elements with fiber cross-sections as well as shell elements for testbed #3. Rayleigh damping was employed to represent the system damping for both testbed structures. Damping coefficients were estimated from the dynamic response of the test structures during experiments, from applying a displacement and suddenly releasing the frame and observing the ring-down as well as through application of optimization of model-based predictions for imposed earthquake shaking [19].

In each modeling instance, the developed FEM was subjected to the earthquake motions imparted to the structure through the base motion generated by the automatically controlled excitation system. The displacements and rotations at the sensor and laser mounting locations were extracted from the FEMs as indicated in Fig. 11.10a and b and post-processed to predict what the sensor system should have measured for each event.

Model-based predictions of sensor measurements for the structures in both testbed #2 and testbed #3 experiments are shown in Fig. 11.10c and d. In these comparisons two features of the FEMs are being tested. First the ability of the model to accurately represent the actual structural response. Secondly, the ability, based on kinematic representation of DDPS system measurements, to translate model-based predictions of structure displacements and rotations into reliable estimates of sensor system performance.

As shown in Fig. 11.10c and d, the FEMs proved to be an effective tool for predicting the expected sensor measurements in both structures. These results exhibit sufficient accuracy to provide confidence in carefully constructed FEMs to predict sensor performance. Having a predictive tool will be important for designing sensor system layouts and extending the sensor designs to other structural configurations including shear wall structures, braced frames, hybrid systems etc. and is thus a key element of the overall technology base.

11.5 Conclusions

In the work presented herein, a new optical sensor for directly measuring transient and residual interstory building drift was described. The capabilities of the DDPS have been successfully demonstrated through extensive experimental testing and through model-based prediction of sensor performance. Exploiting the attributes of optical physics, the sensor is very broad band and can accurately measure time-varying transient drift (TID(t)), peak interstory drift (PID), as well as permanent residual drift (RID) associated with inelastic building response. Thus, the sensor can measure

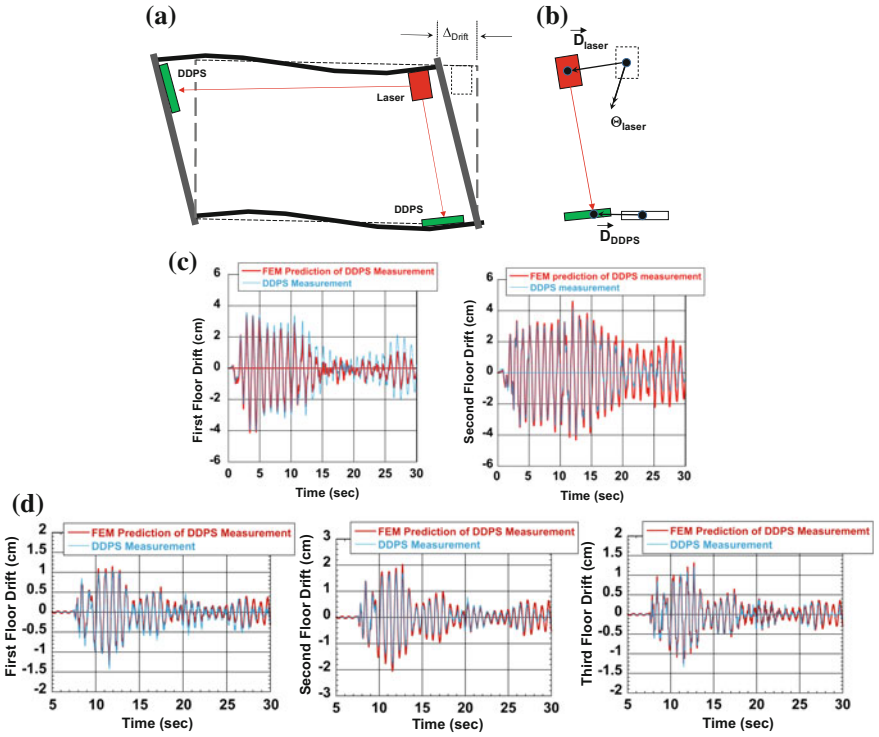

Fig. 11.10 FEM predictions of DDPS measurements. **a** Frame deformed shape from the FEM; **b** extracting displacements and rotations from the FEM at laser and DDPS locations to predict DDPS measurements. Comparison of FEM predictions of sensor measurements with actual DDPS measurements for **c** testbed #2 frame and **d** testbed #3 frame

the full breadth of drift components that are utilized in existing building design codes and standards.

The DDPS system is rapidly approaching readiness for practical application. Figure 11.11 illustrates the evolution of the DDPS technology: the first generation of the DDPS (GEN1) consisted of an assembly of interconnected components and was utilized on Testbed #1 and Testbed #2 (Fig. 11.11a). The second generation of the DDPS (GEN2), included all components integrated on a single circuit board and was utilized on Testbed #3 (Fig. 11.11b). A third generation of the sensor (GEN3), characterized by a simpler and much more compact integrated sensor with a single diode array is undergoing final development at the University of Nevada, Reno (Fig. 11.11c). By modifying the character of the incident laser beam, a single array of diodes can be used and early tests indicate drift displacement measurements with higher accuracy—on the order of 0.05 cm. With this advancement in accuracy, the DDPS is moving towards an ability to measure wind-induced drift in tall buildings, which would provide a secondary function for system identification of as-built structures under ambient vibrations.

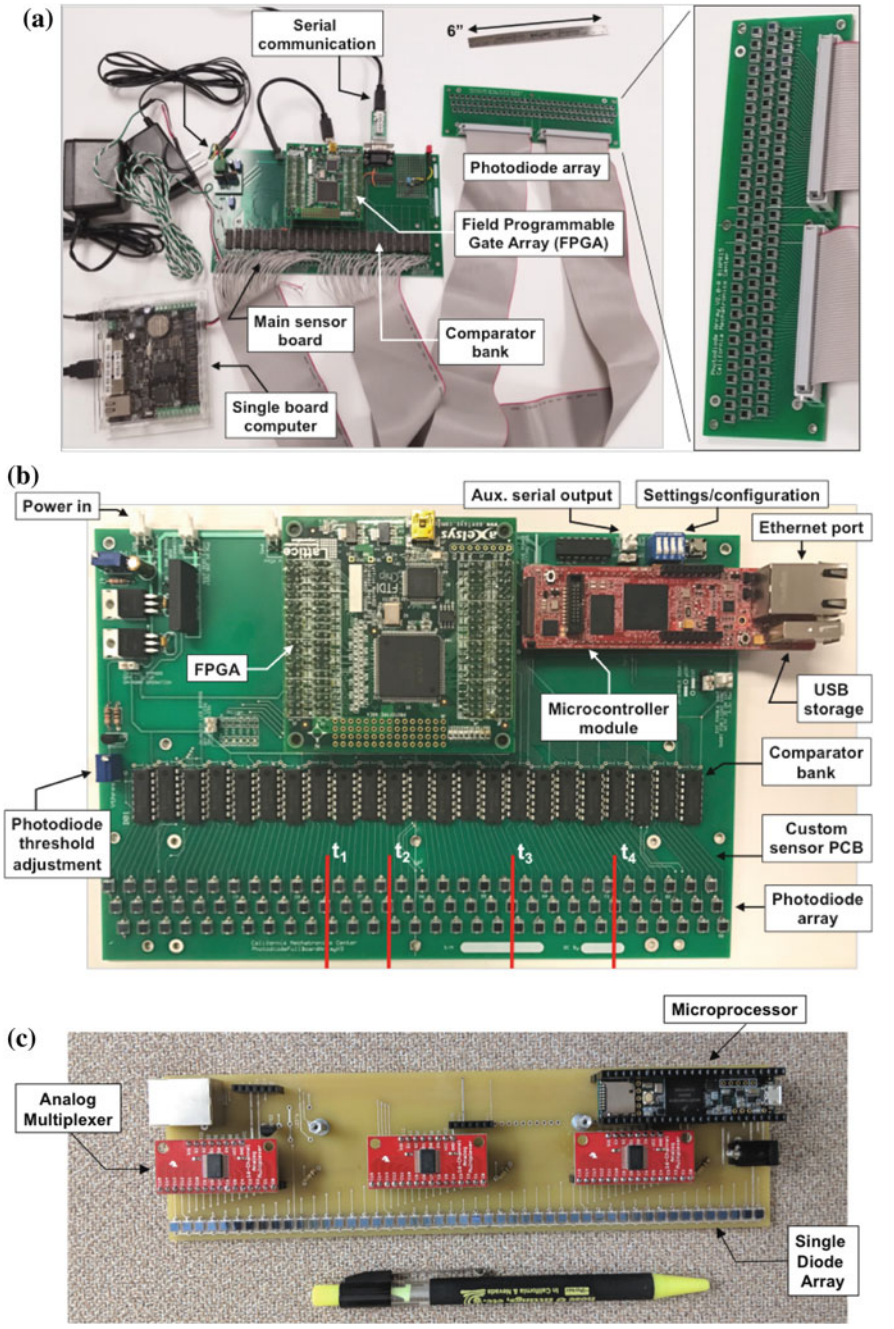

Fig. 11.11 Evolution of DDPS technology. **a** GEN1, interconnected components; **b** GEN2, integrated sensor on a single board; **c** GEN3, compact integrated sensor with single diode array

Final value engineering, to minimize system cost, robustness and packaging/form factor, is underway to achieve the most reliable and cost-effective deployable product. Additionally, the development of deployment "kits" for laser, sensor and mounting hardware, along with mounting guidance to expediently mount the laser and sensor systems on structures, will be required for effective and practical mounting. Improved techniques for addressing local member rotations have recently been identified through model-based simulations [19] and will be experimentally validated. Improved hardware and mounting techniques provide an opportunity to eliminate the need for correction for the local laser rotation, and would be a significant improvement for practical application. Future experimental work will validate the practical mounting concepts.

The DDPS systems can utilize traditional wired connectivity to exfiltrate drift data, but wireless communication nodes that would exfiltrate data across radio frequency (RF) links are under consideration. RF exfiltration to a central hub for access by the IOT would significantly simplify and economize sensor system mounting strategies.

Finally, the first pilot deployment of a DDPS system is being planned on a major building structure in support of S^2HM objectives for the facility. The experimental campaign performed to-date has provided significant experience, but undoubtedly the first full-scale deployment will provide additional insight and lessons-learned.

Acknowledgements The work presented in this paper was supported in part by the U.S. Department of Energy (DOE) Office of Nuclear Safety. This support and the encouragement of Dr. Alan Levin of the Office of Nuclear Safety Research Program is greatly appreciated. The DDPS GEN1 and GEN2 sensors were fabricated at California State University Chico by engineers Jason Coates and Nicholas Repanich. The contributions of Professor Ian Buckle and Dr. Suiwen Wu in designing and conducting the University of Nevada shake table experiments are gratefully acknowledged.

References

1. American Society of Civil Engineers (ASCE) (2005) Seismic design criteria for structures, systems, and components in nuclear facilities. ASCE/SEI 43-05, Reston, VA
2. Bommer JJ, Magenes G, Hancock J, Penazzo P (2004) The influence of strong-motion duration on the seismic response of masonry structures. Bull Earthq Eng 2(1):1–26
3. Celebi M, Sanli A, Sinclair M, Gallant S, Radulescu D (2004) Real-time seismic monitoring needs of a building owner—and the solution: a cooperative effort. Earthq Spectra 20(2):333–346
4. Celebi M (2008) Real-time monitoring of drift for occupancy resumption. In: 14th world conference on earthquake engineering, Beijing China
5. Chen X (1995) Near-field ground motion from the landers earthquake. Report No. EERL 95-02, California Institute of Technology, Earthquake Engineering Research Laboratory, Pasadena, California, USA
6. Chen WM, Bennett KD, Feng J, Wang YP, Huang SL (1998) Laser technique for measuring three dimensional interstory drift. In: Proceedings of the society for photonics and optics, vol 3555, pp 305–310
7. Dai F, Dong S, Kamat VR, Lu M (2011) Photogrammetry assisted measurement of interstory drift for rapid post-disaster building damage reconnaissance. J Nondestruct Eval 30:201
8. Dai F, Lu M (2010) Assessing the accuracy of applying photogrammetry to take geometric measurements on building products. J Constr Eng Manage 136(2):242–250

9. Doebling SW, Farrar CR, Prime MB, Shevitz DW (1996) Damage identification and health monitoring of structural and mechanical systems from changes in their vibration characteristics: a literature review. Los Alamos National Laboratory, Los Alamos, NM
10. Hancock J, Bommer JJ (2006) A state-of-knowledge review of the influence of strong-motion duration on structural damage. Earthq Spectra 22(3):827–845
11. Hou S, Zeng CS, Zhang HB, Ou JP (2018) Monitoring interstory drift in buildings under seismic loading using MEMS inclinometers. Constr Build Mater 185:453–467
12. Hsu TY, Yin RC, Wu YM (2018) Evaluating post-earthquake building safety using economical MEMS seismometers. Sensors 18(5)
13. Lynch JP, Partridge A, Law KH, Kenny TW, Kiremidjian AS, Carryer E (2003) Design of piezoresistive MEMS-based accelerometer for integration with wireless sensing unit for structural monitoring. J Aerosp Eng 16(3):108–114
14. McCallen D, Larsen S (2003) NEVADA—a simulation environment for regional estimation of ground motion and structural response. Report UCRL-ID-152115, Lawrence Livermore National Laboratory
15. McCallen D, Petrone F, Coates J, Repanich N (2017) A laser-based optical sensor for broadband measurements of building earthquake drift. Earthq Spectra 33(4):1573–1598
16. *OpenSees* v 2.5.0 [Computer software]. Berkeley, CA, Pacific Earthquake Engineering Research Center, University of California
17. Pacific Earthquake Engineering Research Center Ground Motion Database (PEER). https://ngawest2.berkeley.edu/
18. Pakzad SN, Fenves GL, Kim S, Culler DE (2008) Design and implementation of scalable wireless sensor network for structural monitoring. J Infrastruct Syst 14(1):89–101
19. Petrone F, McCallen D, Buckle I, Wu S (2018) Direct measurement of building transient and residual drift using an optical sensor system. Eng Struct 176:115–126
20. Sabato A, Niezrecki C, Fortino G (2017) Wireless MEMS-based accelerometer sensor boards for structural vibration monitoring: a review. IEEE Sens J 17(2):226–235
21. Skolnik DA, Kaiser WJ, Wallace JW (2008) Instrumentation for structural health monitoring: measuring interstory drift. In: Proceedings of the 14th world conference on earthquake engineering, 12–17 Oct, Beijing China
22. Skolnik DA, Wallace JW (2010) Critical assessment of interstory drift measurements. J Struct Eng 136:1574–1584
23. Trifunac MD, Ivanovic SS, Todorovska MI (2001) Apparent periods of a building II: time-frequency analysis. J Struct Eng 127:527–537
24. Trifunac MD, Todorovska MI (2001) A note on the usable dynamic range of accelerographs recording translation. J Soil Dyn Earthq Eng 21:275–286
25. Yun F, Yong Z, Weimin C, Rong S, Shanglian H, Bennett KD (1999) Five dimensional interstory drift measurement with cross hair laser. Acta Photonica Sinica 28:1006–1009